ISSN 0915-633X

NATIONAL INSTITUTE FOR FUSION SCIENCE

Passive Shut-Down of ITER Plasma by Be Evaporation

T. Amano

(Received - Jan. 24, 1996)

NIFS-402 Feb. 1996

RESEARCH REPORT
NIFS Series

NAGOYA, JAPAN

Passive Shut-Down of ITER Plasma by Be Evaporation

Tsuneo Amano
National Institute For Fusion Science
464-01 Nagoya.Japan

Abstract

In an accident event where the cooling system of first wall of the ITER fails, the first wall temperature continues to rise as long as the ignited state of the core plasma persists. In this paper, a passive shut-down scheme of the ITER from this accident by evaporated Be from the first wall is examined. It is shown the estimated Be influx 5 10^{24}/sec is sufficient to quench the ignition.

Key Words:
ITER, Passive shutdown of ITER, Beryllium evarpolation

Introduction

In an accident event where the cooling system of the first wall of the ITER[1] fails, the first wall temperature continues to rise as long as the ignited state of the core plasma persists. It is estimated that the Be coated on the first wall will be evaporated at the rate of 5 10^{24}/sec if the first wall temperature reaches 1000K[2]. It is expected that this Be influx cools down the plasma and quench the ignition. In this paper, we examine this passive shut-down scheme of the ITER.

Energy losses in SOL

We assume Be vapors are injected at the rate of N_{Be}=5 10^{24}/sec toward the plasma. The evaporation rate is a very steep function of the first wall temperature and a small temperature increase can double this number. The evaporated Be are ionized in the scrape off layer(SOL) plasma and most of Be ions are swept into the divertor chamber, while a small fraction diffuses into the core plasma. Let the SOL thickness d and the electron density before the Be injection n_{es} and temperature T. SI unit is used except the temperature is measured in eV.
Be ion density $n_{Be,S}$ in SOL is obtained from a balance of Be input into the SOL and parallel particle loss along field lines:

[1] $n_{Be,S} = N_{Be}/(2\ 2\pi\sqrt{\varepsilon}\ a\ d\ v/q)$

where a is the minor radius of the plasma, ε is the elipticity and v is the thermal speed of the Be ions and q is the safty factor in the SOL. Figure[1] shows the Be ion density vs. SOL temperature. Here we take a=3m, ε=1.6 , d=0.2m and q=3..

The ionization degree and ionization and energy losses are calculated by using APDAK atomic physics package[3]. This package is able to calculate the ionization and recombination rates and radiation energy losses for any atomic species. The accuracy of the code for Be case is compared to more elaborate atomic physics calculations in Fig.[12] of reference[4]. The agreement is very good above the electron temperature T>15 eV. Below 15eV, radiation reduction due to collisional de-excitation is important which the APDAK code does not take into account.

The average charge number of the Be ions calculated by the code is shown in Fig.[2]. Here we take into account particle losses along the field lines in the Corona equilibrium calculation.

Total SOL electron density is given as

[2] $n_{e,tot}=n_{e,S}+<Z>n_{Be,S}$,

which is plotted in Fig.[3]

A Be atom has 4 electrons whose ionization potential are (9.32,18.21,153.89,217.71) eV. The Be is fully ionized for T>50eV, then the energy required to ionize 5 10^{24}/sec Be influx amounts to 320MW which is more than the alpha particle heating power (300MW) in the standard ITER operations.

The energy required for Be ions and electrons to gain the temperature T is given by

[3] $Etherm = N_{Be}\ (1+<Z>)\ 1.5k_0T$.

The energy flow to the divertor chamber is given by

[4] $Eflow = (n_{e,tot} + n_{Be,S})\ 2\ v\ /\ q\ 2\pi a\sqrt{\varepsilon}\ d\ 1.5k_0T$,

where the heat conduction energy losses are not included. If we neglect $n_{e,S}$ in Eq.[4], we notice Eflow=Etherm.

Ionization energy loss by Be is shown in Fig.[4] as a function of T. Eflow and Etherm are shown in Figs.[5] and [6].

The energy loss due to radiation processes is obtained from

[5] $Erad = n_{e,tot}\ n_{Be,s}\ 2\pi a\sqrt{\varepsilon}\ 2\pi R_0\ d\ Frad(T)$

where R_0=8m is the major radius and Frad(T) is the Be radiation energy loss for unit electron and Be densities. Frad(T) and Erad are plotted in Fig.[7] and Fig[8],respectively.

Total energy loss Eion+Eflow+Etherm+Erad is plotted in Fig.[9]. The energy loss in the SOL exceeds 300MW/sec except inside a narrow region around T≈10eV. As noted earlier, the APDAK calculation gives overestimate of the radiation loss in this region. Fig.[10] shows the energy loss in the SOL around T=10eV. Here the reduction of the radiation energy loss by a factor of about 200 due to the collisional de-excitation is taken into account. From Fig.[10], it looks there may exist an equilibrium with $T \approx 10eV$ and $n_e \approx 2\ 10^{20}/m^3$ (See Fig.[3]), in the presence of the heating power 300MW from the core plasma. However, such a low temperature SOL can not sustain H-mode and the H-L transition will kill the ignition.

Be influx in to core plasma

Let us now estimate the Be diffusion flux into the core plasma. As for the cross field diffusion coefficient of Be ions in the SOL, we consider the (1) Bohm diffusion and (2) neoclassical diffusion.

The influx of the Be into the core plasma is estimated as

[6] $N_{Be,p} = D dn_{Be,S}/dr\ S = D\ n_{Be,S}/d\ 2\pi R_0\ 2\pi a \sqrt{\varepsilon}$

where D is the diffusion coefficient.

As the maximum allowed Be fraction for the ignition, we take 0.1. For the core ion density $10^{20}/m^3$, the maximum allowed Be density is $10^{19}/m^3$.

Define the critical Be fraction to penetrate into the core plasma by

[7] $Be,limit = 10^{19}/(N_{Be}\ \tau_p/(\pi a^2 \sqrt{\varepsilon}\ 2\pi R_0)) = 0.0001$

where the denominator means the Be density in the core plasma when all the Be ions enter the core plasma. τ_p is the particle confinement time for which we take 5 seconds(same as the energy confinement time). Fig.[11] shows the Be fraction to enter the core plasma $N_{Be,p}/N_{Be}$ for the Bohm diffusion coefficient $D=T/100(m^2/sec)$. In the figure, lower line is the critical Be limit line.

The same calculation is done for the case of neoclassical diffusion case. Fig.[12] shows the neoclassical Hazeltine-Hinton diffusion coefficient.[5] Fig.[13] shows the Be fraction to enter the core plasma for the neoclassical diffusion coefficient case. The lower line is the critical Be fraction limit line.

From Fig.[11] and [13], we conclude that the Be diffusion into the core plasma is sufficiently large to quench the ignition even for neoclassical diffusion.

Discussion

We have shown that the energy loss by the Be ions exceeds the alpha particle heating power, if the SOL temperature is greater than about 20eV.(Fig.[10]). We could not exclude a possibility that an equilibrium can exist where the SOL temperature is about 10eV. However, such low temperature SOL will cause the H-L transition which quenches the ignition.

The diffusion of Be ions into the core plasma can also cause the quenching of the ignition. By assuming 10% Be concentration in the core plasma inhibits the ignition, we have shown that the Be diffusion is sufficiently large for the Bohm diffusion coefficient and exceeds the fatal Be concentration 10% for every temperature range.(Fig.[11]) Even the neoclassical diffusion is sufficiently large. (Fig.[12]).

We have deliberately estimated the effects of Be influx as conservatively as possible ,since we are concerned with safety of the ITER :
(1) SOL width is taken d=0.2m. In the standard ITER condition, d is about 0.05m.
(2) Heat conduction loss is neglected.
(3) Power input to the SOL is taken 300MW. In fact , it is about 230MW after subtracting Bremstrahlung loss.
(4) The particle confinement is taken 5 sec which is the same as the ITER's energy confinement time. Usually, the particle confinement time is several time greater than the energy confinement time.
(5) The fatal Be concentration to quench the ITER ignition is taken as 10%. The "PRETOR" simulations give the Be fatal concentration less than 5%.

Acknowledgments

This work was done during the author's stay in the ITER San Diego Joint Work Site in 1965. He wishes to thank for the financial support for Japanese Government Ministry of Education for this stay.
He wishes to thank Dr. Shimomura for suggesting the problem and many useful discussions with the ITER safety group members.

References

1. ITER Interim Design Report. June 1995.

2. Private communication from Dr. Shimomura and Dr. Bartels.
3. R. Hulse, Nucl. Techn/Fusion 3(1983) 259.
4. D.E. Post, J. Nucl. Mater. 220-222(1995) 143.
5. F.L. Hinton and R.D. Hazeltine, Rev. Mod. Phys. 48, 239

Figure Captions.

Figure 1. SOL Be ion density($10^{20}/m^3$) as a function of the SOL temperature.

Figure 2. The average charge number of the Be ions as a function of the SOL temperature.

Figure 3. The sol total electron density as a function of the SOL temperature.

Figure 4. Be ionization energy loss as a function of the SOL temperature.

Figure 5. Flow energy loss to the divertor as a function of the SOL temperature.

Figure 6 Thermal energy loss as a function of the SOL temperature.

Figure 7. Be radiation energy loss per unit Be and electron densities as a function of the SOL temperature.

Figure 8. Radiation energy loss as a function of the SOL temperature.

Figure 9. Total energy loss as a function of the SOL temperature.

Figure 10. Total energy loss around T=10eV. Here the reduction of the radiation loss due to collisional de-excitation is taken into account.

Figure 11. Be fraction to enter the core plasma as a function of the SOL temperature. Bohm diffusion case. Lower curve indicates the fatal fraction of Be in the plasma to quench the ignition.

Figure 12. Neoclassical diffusion coefficient in the SOL.

Figure 13. Be fraction to enter the core plasma. Neoclassical diffusion case. Lower curve indicates the fatal fraction of Be in the plasma to quench the ignition.

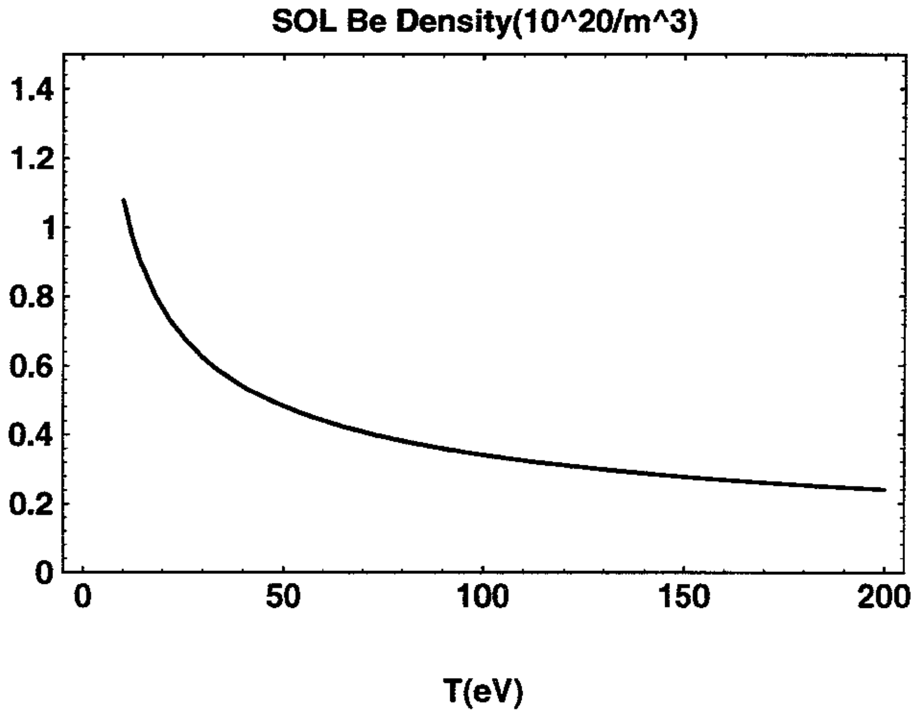
SOL Be Density(10^20/m^3)
1.4
1.2
1
0.8
0.6
0.4
0.2
0
0
50
100
150
200
T(eV)

Fig.1

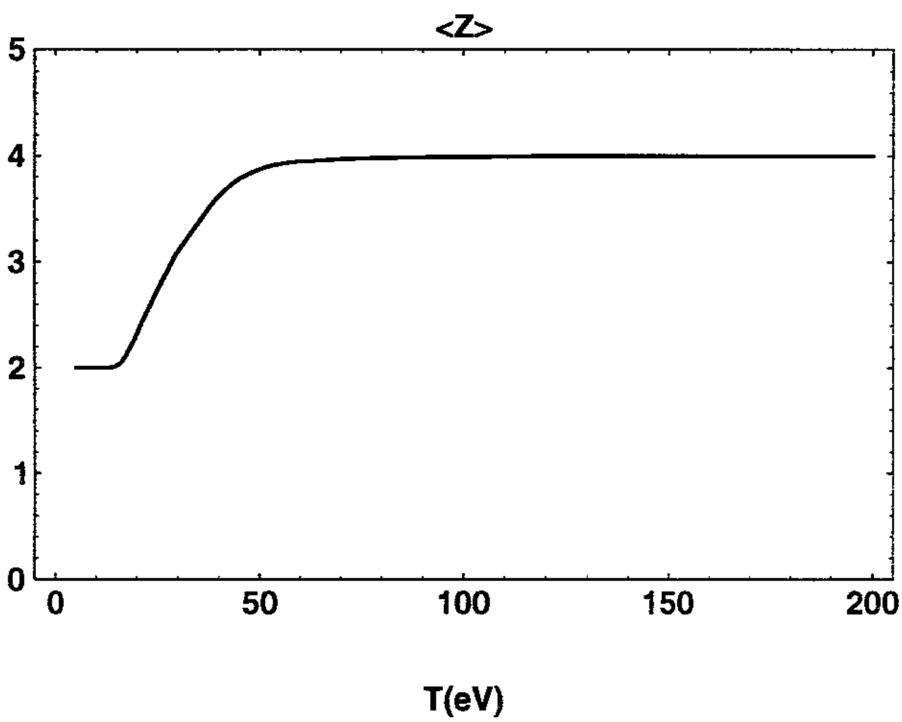
<Z>
5
4
3
2
1
0
0
50
100
150
200
T(eV)

Fig.2

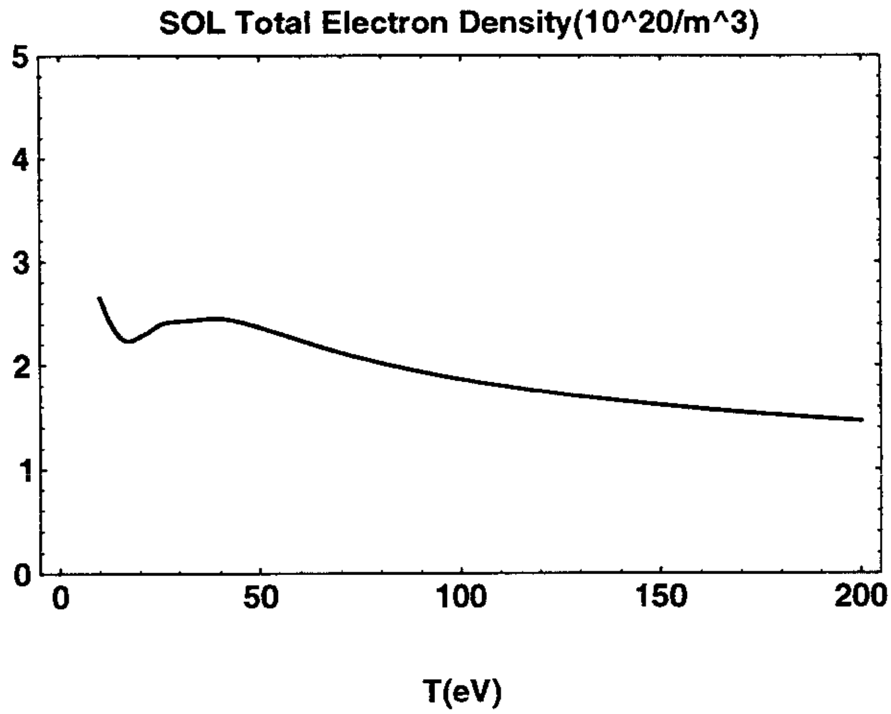
SOL Total Electron Density(10^20/m^3)
5
4
3
2
1
0
0
50
100
150
200
T(eV)

Fig.3

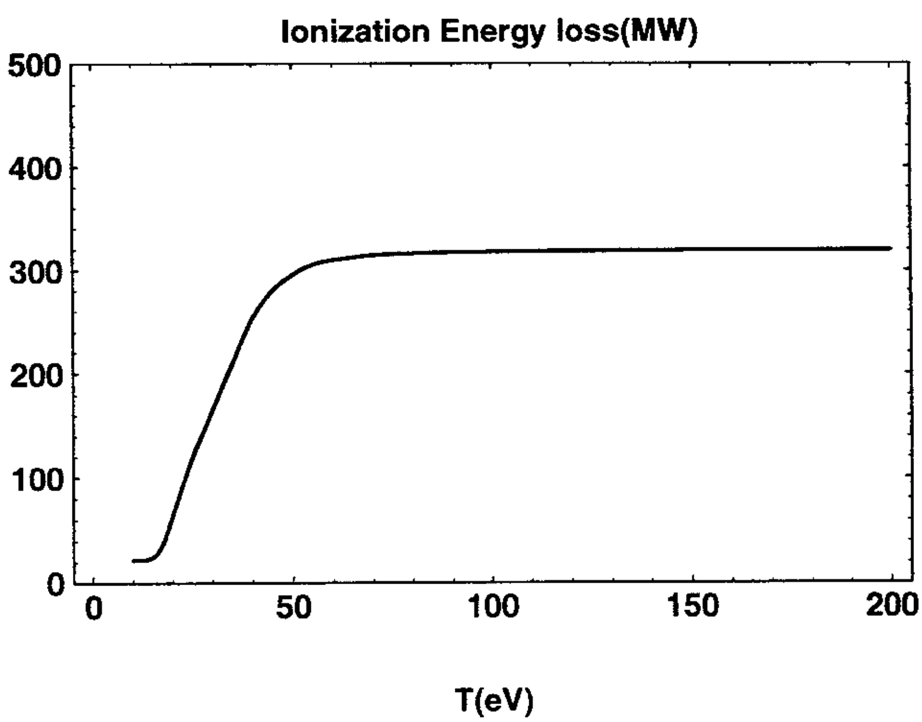
Ionization Energy loss(MW)
500
400
300
200
100
0
0
50
100
150
200
T(eV)

Fig.4

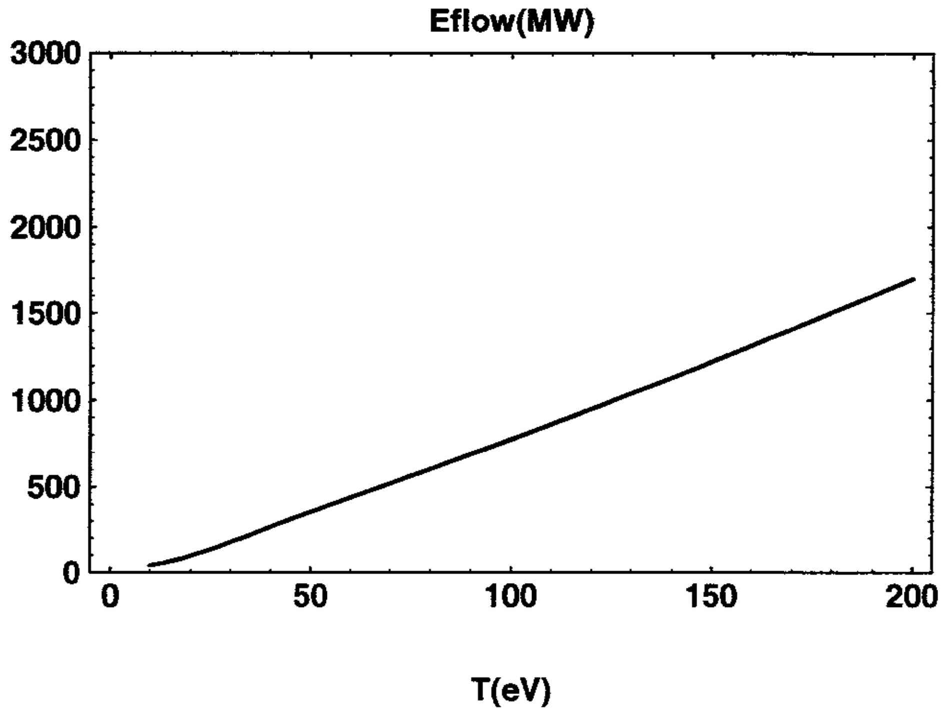
Eflow(MW)
3000
2500
2000
1500
1000
500
0
0
50
100
150
200
T(eV)
Fig.5

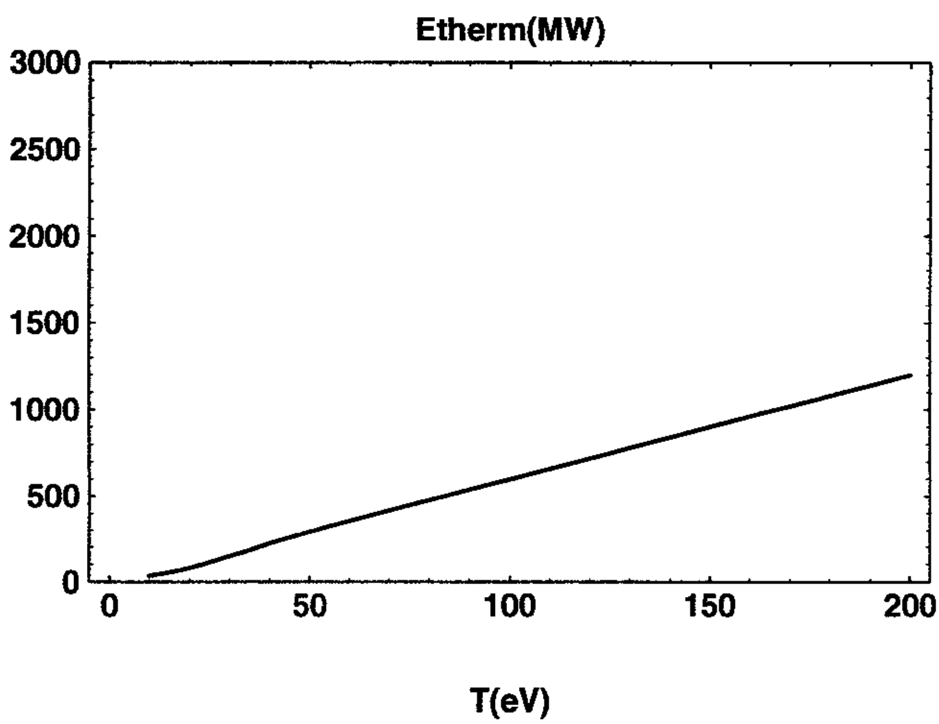
Etherm(MW)
3000
2500
2000
1500
1000
500
0
0
50
100
150
200
T(eV)
Fig.6

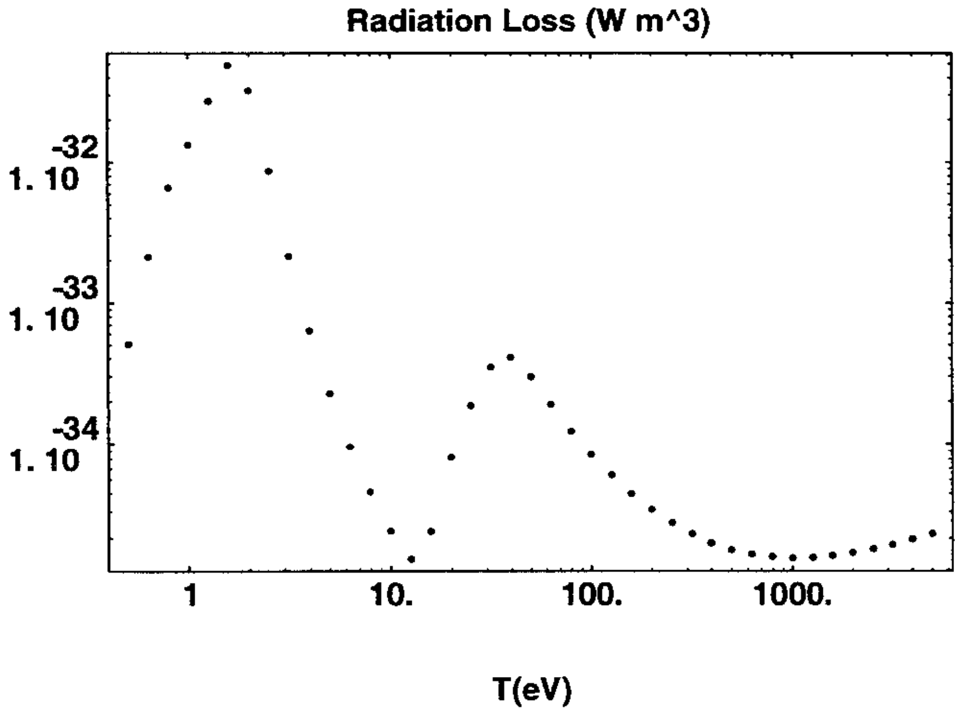
Radiation Loss (W m^3)
-32
1. 10
-33
1. 10
-34
1. 10
1
10.
100.
1000.
T(eV)

Fig.7

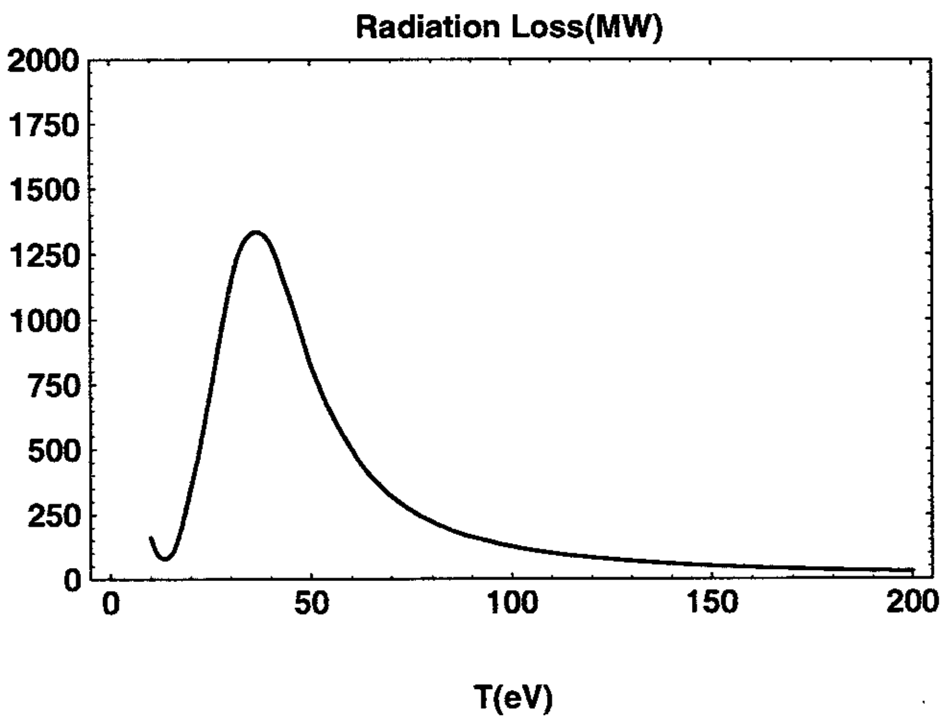
Radiation Loss(MW)
2000
1750
1500
1250
1000
750
500
250
0
0
50
100
150
200
T(eV)

Fig.8

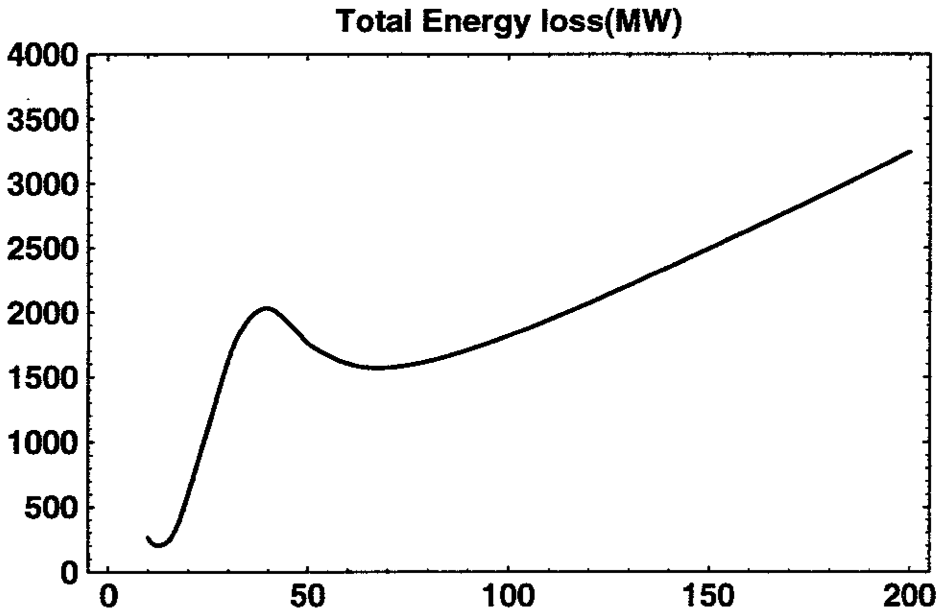

T(eV)

Fig.9

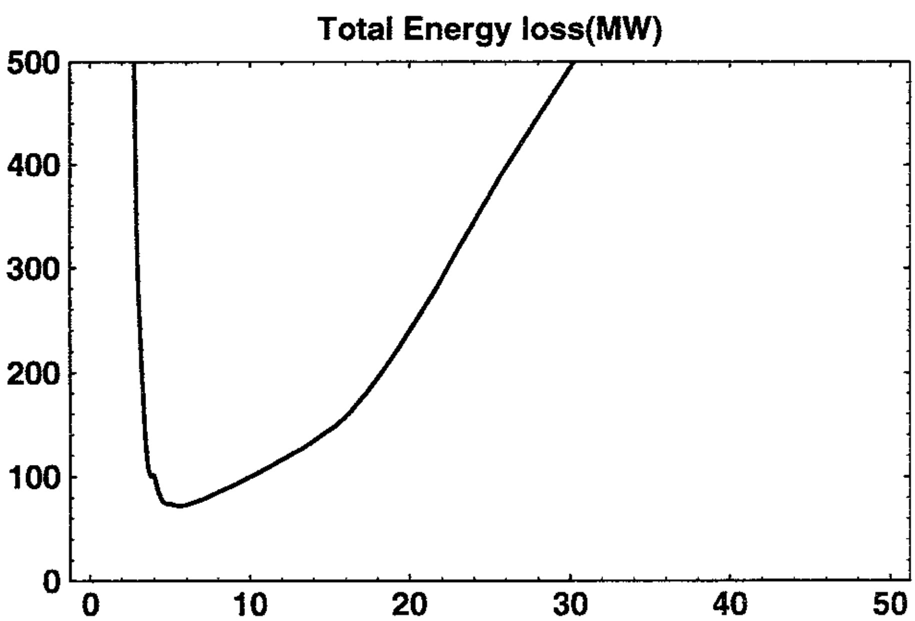

T(eV)

Fig.10

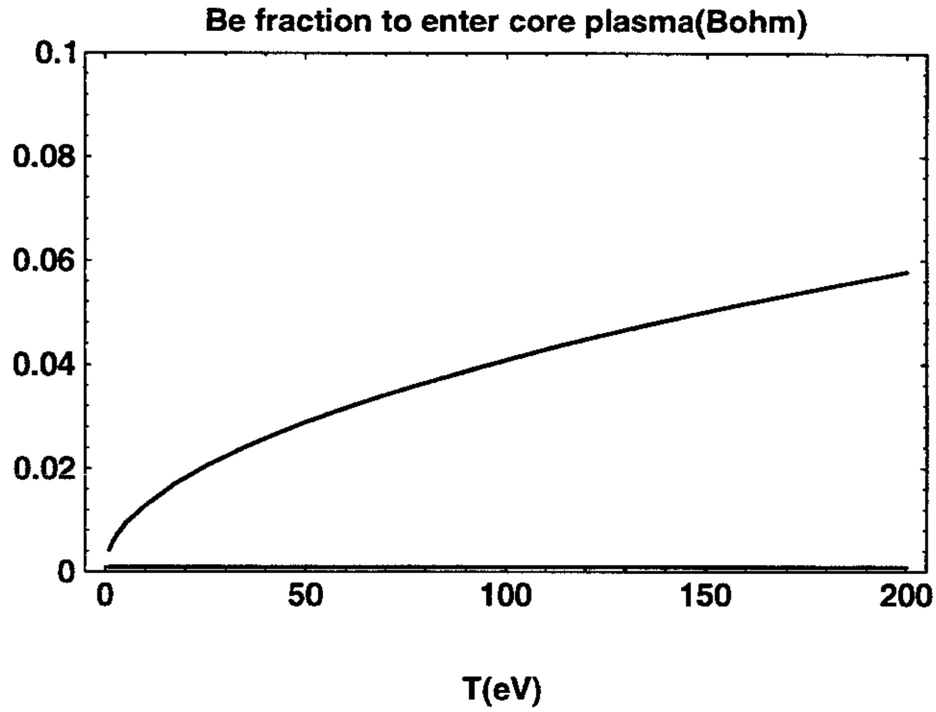
Be fraction to enter core plasma(Bohm)
0.1
0.08
0.06
0.04
0.02
0
0
50
100
150
200
T(eV)

Fig.11

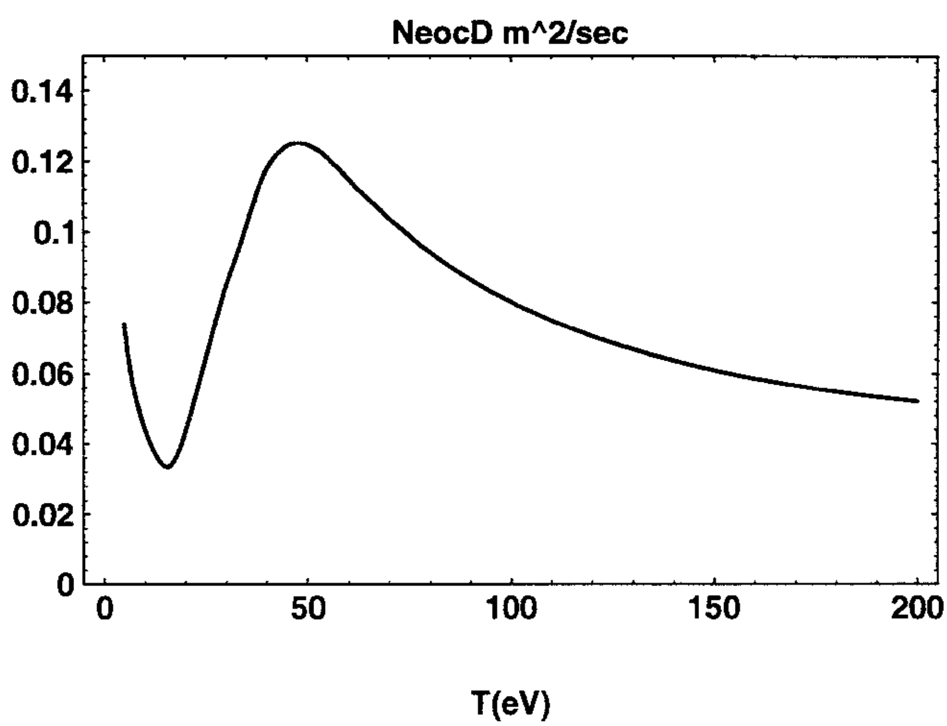
NeocD m^2/sec
0.14
0.12
0.1
0.08
0.06
0.04
0.02
0
0
50
100
150
200
T(eV)

Fig12

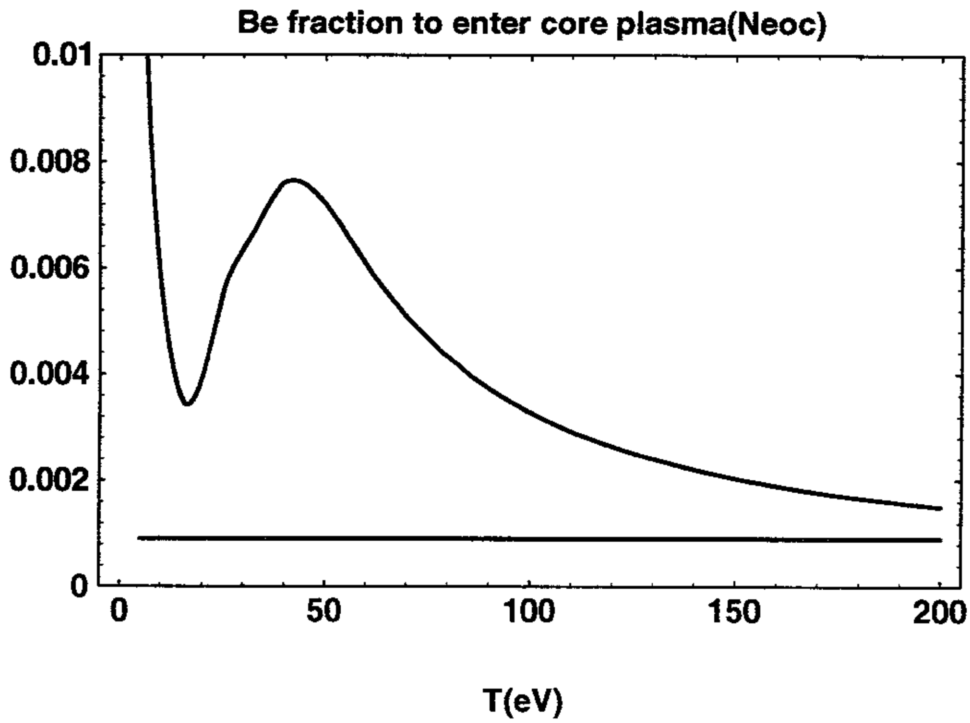
Be fraction to enter core plasma(Neoc)
0.01
0.008
0.006
0.004
0.002
0
0
50
100
150
200
T(eV)
Fig.13

Recent Issues of NIFS Series

NIFS-355 H. Sugama and W. Horton,
Neoclassical and Anomalous Transport in Axisymmetric Toroidal Plasmas with Electrostatic Turbulence; May 1995

NIFS-356 N. Ohyabu
A New Boundary Control Scheme for Simultaneous Achievement of H-mode and Radiative Cooling (SHC Boundary); May 1995

NIFS-357 Y. Hamada, K.N. Sato, H. Sakakita, A. Nishizawa, Y. Kawasumi, R. Liang, K. Kawahata, A. Ejiri, K. Toi, K. Narihara, K. Sato, T. Seki, H. Iguchi, A. Fujisawa, K. Adachi, S. Hidekuma, S. Hirokura, K. Ida, M. Kojima, J. Koong, R. Kumazawa, H. Kuramoto, T. Minami,. M. Sasao, T. Tsuzuki, J.Xu, I. Yamada, and T. Watari,
Large Potential Change Induced by Pellet Injection in JIPP T-IIU Tokamak Plasmas; May 1995

NIFS-358 M. Ida and T. Yabe,
Implicit CIP (Cubic-Interpolated Propagation) Method in One Dimension; May 1995

NIFS-359 A. Kageyama, T. Sato and The Complexity Simulation Group,
Computer Has Solved A Historical Puzzle: Generation of Earth's Dipole Field; June 1995

NIFS-360 K. Itoh, S.-I. Itoh, M. Yagi and A. Fukuyama,
Dynamic Structure in Self-Sustained Turbulence; June 1995

NIFS-361 K. Kamada, H. Kinoshita and H. Takahashi,
Anomalous Heat Evolution of Deuteron Implanted Al on Electron Bombardment; June 1995

NIFS-362 V.D. Pustovitov,
Suppression of Pfirsch-schlüter Current by Vertical Magnetic Field in Stellarators; June 1995

NIFS-363 A. Ida, H. Sanuki and J. Todoroki
An Extended K-dV Equation for Nonlinear Magnetosonic Wave in a Multi-Ion Plasma; June 1995

NIFS-364 H. Sugama and W. Horton
Entropy Production and Onsager Symmetry in Neoclassical Transport Processes of Toroidal Plasmas; July 1995

NIFS-365 K. Itoh, S.-I. Itoh, A. Fukuyama and M. Yagi,
On the Minimum Circulating Power of Steady State Tokamaks; July 1995

NIFS-366 K. Itoh and Sanae-I. Itoh,
The Role of Electric Field in Confinement; July 1995

NIFS-367 F. Xiao and T. Yabe,
A Rational Function Based Scheme for Solving Advection Equation; July 1995

NIFS-368 Y. Takeiri, O. Kaneko, Y. Oka, K. Tsumori, E. Asano, R. Akiyama, T. Kawamoto and T. Kuroda,
Multi-Beamlet Focusing of Intense Negative Ion Beams by Aperture Displacement Technique; Aug. 1995

NIFS-369 A. Ando, Y. Takeiri, O. Kaneko, Y. Oka, K. Tsumori, E. Asano, T. Kawamoto, R. Akiyama and T. Kuroda,
Experiments of an Intense H- Ion Beam Acceleration; Aug. 1995

NIFS-370 M. Sasao, A. Taniike, I. Nomura, M. Wada, H. Yamaoka and M. Sato,
Development of Diagnostic Beams for Alpha Particle Measurement on ITER; Aug. 1995

NIFS-371 S. Yamaguchi, J. Yamamoto and O. Motojima;
A New Cable -in conduit Conductor Magnet with Insulated Strands; Sep. 1995

NIFS-372 H. Miura,
Enstrophy Generation in a Shock-Dominated Turbulence; Sep. 1995

NIFS-373 M. Natsir, A. Sagara, K. Tsuzuki, B. Tsuchiya, Y. Hasegawa, O. Motojima,
Control of Discharge Conditions to Reduce Hydrogen Content in Low Z Films Produced with DC Glow; Sep. 1995

NIFS-374 K. Tsuzuki, M. Natsir, N. Inoue, A. Sagara, N. Noda, O. Motojima, T. Mochizuki, I. Fujita, T. Hino and T. Yamashina,
Behavior of Hydrogen Atoms in Boron Films during H_2 and He Glow Discharge and Thermal Desorption; Sep. 1995

NIFS-375 U. Stroth, M. Murakami, R.A. Dory, H. Yamada, S. Okamura, F. Sano and T. Obiki,
Energy Confinement Scaling from the International Stellarator Database; Sep. 1995

NIFS-376 S. Bazdenkov, T. Sato, K. Watanabe and The Complexity Simulation Group,
Multi-Scale Semi-Ideal Magnetohydrodynamics of a Tokamak Plasma; Sep. 1995

NIFS-377 J. Uramoto,
Extraction of Negative Pionlike Particles from a H2 or D2 Gas Discharge Plasma in Magnetic Field; Sep. 1995

NIFS-378 K. Akaishi,
Theoretical Consideration for the Outgassing Characteristics of an Unbaked Vacuum System; Oct. 1995

NIFS-379 H. Shimazu, S. Machida and M. Tanaka,
Macro-Particle Simulation of Collisionless Parallel Shocks; Oct. 1995

NIFS-380 N. Kondo and Y. Kondoh,
Eigenfunction Spectrum Analysis for Self-organization in Dissipative Solitons; Oct. 1995

NIFS-381 Y. Kondoh, M. Yoshizawa, A. Nakano and T. Yabe,
Self-organization of Two-dimensional Incompressible Viscous Flow in a Friction-free Box; Oct. 1995

NIFS-382 Y.N. Nejoh and H. Sanuki,
The Effects of the Beam and Ion Temperatures on Ion-Acoustic Waves in an Electron Beam-Plasma System; Oct. 1995

NIFS-383 K. Ichiguchi, O. Motojima, K. Yamazaki, N. Nakajima and M. Okamoto
Flexibility of LHD Configuration with Multi-Layer Helical Coils; Nov. 1995

NIFS-384 D. Biskamp, E. Schwarz and J.F. Drake,
Two-dimensional Electron Magnetohydrodynamic Turbulence; Nov. 1995

NIFS-385 H. Kitabata, T. Hayashi, T. Sato and Complexity Simulation Group,
Impulsive Nature in Collisional Driven Reconnection; Nov. 1995

NIFS-386 Y. Katoh, T. Muroga, A. Kohyama, R.E. Stoller, C. Namba and O. Motojima,
Rate Theory Modeling of Defect Evolution under Cascade Damage Conditions:The Influence of Vacancy-type Cascade Remnants and Application to the Defect Production Chracterization by Microstructural Analysis; Nov. 1995

NIFS-387 K. Araki, S. Yanase and J. Mizushima,
Symmetry Breaking by Differential Rotation and Saddle-node Bifurcation of the Thermal Convection in a Spherical Shell; Dec. 1995

NIFS-388 V.D. Pustovitov,
Control of Pfirsch-Schlüter Current by External Poloidal Magnetic Field in Conventional Stellarators: Dec. 1995

NIFS-389 K. Akaishi,
On the Outgassing Rate Versus Time Characteristics in the Pump-down of an Unbaked Vacuum System; Dec. 1995

NIFS-390 K.N. Sato, S. Murakami, N. Nakajima, K. Itoh, *Possibility of Simulation Experiments for Fast Particle Physics in Large Helical Device (LHD)*; Dec. 1995

NIFS-391 W.X.Wang, M. Okamoto, N. Nakajima, S. Murakami and N. Ohyabu,
A Monte Carlo Simulation Model for the Steady-State Plasma in the Scrape-off Layer; Dec. 1995

NIFS-392 Shao-ping Zhu, R. Horiuchi, T. Sato and The Complexity Simulation Group,
Self-organization Process of a Magnetohydrodynamic Plasma in the Presence of Thermal Conduction; Dec. 1995

NIFS-393 M. Ozaki, T. Sato, R. Horiuchi and the Complexity Simulation Group
Electromagnetic Instability and Anomalous Resistivity in a Magnetic Neutral Sheet; Dec. 1995

NIFS-394 K. Itoh, S.-I Itoh, M. Yagi and A. Fukuyama,
Subcritical Excitation of Plasma Turbulence; Jan. 1996

NIFS-395 H. Sugama and M. Okamoto, W. Horton and M. Wakatani,
Transport Processes and Entropy Production in Toroidal Plasmas with Gyrokinetic Eletromagnetic Turbulence. Jan. 1996

NIFS-396 T. Kato, T. Fujiwara and Y. Hanaoka,
X-ray Spectral Analysis of Yohkoh BCS Data on Sep. 6 1992 Flares - Blue Shift Component and Ion Abundances -; Feb. 1996

NIFS-397 H. Kuramoto, N. Hiraki, S. Moriyama, K. Toi, K. Sato, K. Narihara, A. Ejiri, T. Seki and JIPP T-IIU Group,
Measurement of the Poloidal Magnetic Field Profile with High Time Resolution Zeeman Polarimeter in the JIPP T-IIU Tokamak; Feb. 1996

NIFS-398 J.F. Wang, T. Amano, Y. Ogawa, N. Inoue,
Simulation of Burning Plasma Dynamics in ITER; Feb. 1996

NIFS-399 K. Itoh, S-I. Itoh, A. Fukuyama and M. Yagi,
Theory of Self-Sustained Turbulence in Confined Plasmas; Feb. 1996

NIFS-400 J. Uramoto,
A Detection Method of Negative Pionlike Particles from a H2 Gas Descharge Plasma; Feb. 1996

NIFS-401 K.Ida. J.Xu, K.N.Sato, H.Sakakita and JIPP TII-U group,
Fast Charge Exchange Spectroscopy Using a Fabry-Perot Spectrometer in the JIPP TII-U Tokamak; Feb. 1996

NIFS-402 T. Amano,
Passive Shut-Down of ITER Plasma by Be Evaporation; Feb. 1996